Effective model based on QCD with gluon condensate

Hiroaki Kohyama
Department of Physics, National Taiwan University, Taipei 10617, Taiwan
(Dated: June 3, 2016)

We construct the effective model based on QCD with gluon condensate. Under the assumption that the gluons are condensed with the sharp momentum peak in the momentum space, we formulate the effective field theory incorporating both the gluon condensate and the chiral condensate, then study the phase transition on temperature and chemical potential plane with respect to two condensates. We find that the condensates decrease with increasing temperature, which is reliable tendency on the condensate being consistent with the argument of the asymptotic behavior.

PACS numbers: 11.10.Wx, 12.38.-t, 12.40.-y

arXiv:1606.00673v1 [hep-ph] 2 Jun 2016

I. INTRODUCTION

The first principle theory for quarks and gluons is quantum chromodynamics (QCD), whose goal is to explain all the phenomena relating to the strong interaction. However, it is known to be difficult since usual perturbative technologies in the quantum theory calculations hardly works for low energy physics in which nonperturbative effect dominates the system then complicates the analyses. One of characteristic features is nontrivial gluon and chiral condensates in the nonperturbatively correlated system due to the strong interaction. It is challenging to derive the condensates relying on the perturbative quantum field analyses, then one usually has to use some effective models of QCD for the sake of describing the low energy physics, such as properties of hadrons.

There has been a lot of investigations on low energy phenomena based on various effective theories treating the gluon and chiral condensates. The instanton includes the gluon condensate though the solution to the classical field equation [1], and various applications have been done [2–5]. QCD sum rule is formulated by the expansion of the correlation functions in the vacuum condensates [6], which is as well widely used for many applications [7–9]. The Schwinger-Dyson equations (SDE) are the equations for the exact correlation functions of fields [10], and there has been devoted to a lot of analyses [11–14]. The Nambu–Jona-Lasinio (NJL) model [15] is constructed using the analogy with the BCS theory for superconductivity [16]; the model studies the hadron properties based on the back ground chiral condensate [17–21]. An extension of the NJL model has been made in [22] where the Polyakov-loop contribution is incorporated into the chiral dynamics, and extensive analyses on both the chiral and gluon loop condensates have been performed in the Polyakov loop NJL (PNJL) model [23]. Thus the issues on the gluon and chiral condensates are essential in the study of hadron physics, there we believe these two condensates are intimately related to each other.

In this paper, we construct the effective model based on QCD by postulating that gluons form the condensation whose momenta have the sharp peak at the QCD scale [24]. The speculation is inspired by the experiments of the momentum in the Bose Einstein condensate (BEC) state where the clear peak in the momentum distribution is actually observed. We then consider the analogy between the BEC state and the gluon condensed state as done in a chiral effective model motivated from the BCS analogy. To be more concrete, we are going to formulate the gap equation for the gluon condensate from the QCD under the above mentioned assumption with gluon condensate. It may be important to remark that the solution of the gap equation for the gluon condensate at high temperature behaves badly, since many bosons can unlimitedly occupy the same point due to the statistical property of bosonic fields to cause the catastrophic situation in the gap equation. Therefore the special attention should be paid when one treats the solution at high temperature near the phase transition. However, although the high temperature results do not behave nicely, meaning that the plots deviate from the expected ones from the BEC experimental data, we find that the tendency of the gluon condensate shows physically reliable feature as will be presented later. We then proceed the analyses based on the gluon condensate by using the gap equation with simple form. Here the purpose of this letter is twofold: first, to construct the QCD motivated effective model based on the anzatz of the gluon condensate and second, to see how the obtained model describes the thermodynamic properties and how it affects to the chiral condensate.

The paper is organized following. We formulate the gap equations for the gluons, quarks, and coupled system in Sec. II. The numerical solutions for the gap equations in the separate models are shown in Sec. III. Secs. IV and V are devoted to the investigations on the thermodynamic quantities and the phase structure in the coupled model. The conclusions and some subsidiary calculations are given in Sec. VI and Appendices.

II. QCD WITH GLUON CONDENSATE

Starting from the QCD Lagrangian, we are going to evaluate the effective potential under the hypothetical situation of the condensed gluons. Thereafter the gap

equations for the gluon and chiral condensates, and their coupled equation are derived.

A. Gluon gap equation

The Lagrangian for gluon is given by

$$\mathcal{L}_{\rm g} = \mathcal{L}_{\rm g}^0 + \mathcal{L}_{\rm g}^3 + \mathcal{L}_{\rm g}^4, \tag{1}$$

$$\mathcal{L}_{\rm g}^0 = -\frac{1}{4}(\partial_\mu A_\nu^a - \partial_\nu A_\mu^a)^2, \tag{2}$$

$$\mathcal{L}_{\rm g}^3 = -g f^{abc}(\partial_\mu A_\nu^a) A^{\mu b} A^{\nu c}, \tag{3}$$

$$\mathcal{L}_{\rm g}^4 = -\frac{1}{4} g^2 (f^{eab} A_\mu^a A_\nu^b)(f^{ecd} A^{\mu c} A^{\nu d}), \tag{4}$$

where A_μ is the gluon field, g is the coupling constant for the strong interaction and f^{abc} is the structure constant with respect to the SU(3) color system.

The effective potential can be evaluated through the relation, $\Omega_{\rm g} \equiv -\ln \mathcal{Z}/V$ with the partition function $\mathcal{Z}$ and the volume of the system V, whose explicit form becomes

$$\Omega_{\rm g} = -\frac{1}{V}\int {\rm d}^4x\ \langle \mathcal{L}_{\rm g}\rangle - \frac{i}{2V}\ln\det\left\langle -\frac{\delta^2 \mathcal{L}_{\rm g}}{\delta A_\mu^a \delta A_\nu^b}\right\rangle + \cdots \tag{5}$$

where the bracket expresses the expectation value of the quantity, $O_{\rm ex} \equiv \langle O\rangle$.

Before proceeding the calculation of the effective potential, we present the main assumption on the gluon fields here. The characteristic treatment of the gluon field is that we assume the fields are condensed then have non-zero expectation value. The usual Feynman rule for the two-point function on the gluon is the amplitude

$$\left\langle A_\mu^a(x) A_\nu^b(x)\right\rangle_{\rm p} = g_{\mu\nu}\delta^{ab}\int \frac{{\rm d}^4p}{(2\pi)^4}\frac{-i}{p^2+i\epsilon}. \tag{6}$$

calculated from the perturbative gluon propagator. The amplitude badly diverges due to the loop integral, then we need to perform the renormalization so that one gets finite physical predictions. Here, we postulate that the exact renormalized two-point function has the following expectation value,

$$\langle A_\mu^a(x) A_\nu^b(x)\rangle_{\rm ex} = g_{\mu\nu}\delta^{ab}\phi_{\rm g}, \tag{7}$$

which is made to be finite by virtue of the renormalization, and we call the quantity $\phi_{\rm g}$ as the gluon condensate. Eq.(7) is the key hypothesis employed in this paper.

Let us now carry out the evaluation of the effective potential with the help of the above mentioned ingredients. The non-zero contribution in the first term of Eq. (5) stems from the four-point interaction [24],

$$\langle \mathcal{L}_{\rm g}\rangle = -72 g^2 \phi_{\rm g}^2. \tag{8}$$

Note that $\langle \mathcal{L}_{\rm g}^3\rangle = 0$ due to the antisymmetric property of the structure constant f^{abc}. It is also straightforward to evaluate the second term in Eq. (5), which reads

$$\begin{aligned}
&\frac{-i}{2V}\ln\det\left\langle -\frac{\delta^2\mathcal{L}_{\rm g}}{\delta A_\mu^a \delta A_\nu^b}\right\rangle \\
&= \frac{-i}{2V}\ln\det\left[g^{\mu\nu}\delta^{ab}\left(-p^2 + 9g^2\phi_{\rm g}\right)\right] \\
&= -16i\int\frac{{\rm d}^4p}{(2\pi)^4}\ln\left[-p^2 + M_{\rm g}^2\right],
\end{aligned} \tag{9}$$

with the effective gluon mass $M_{\rm g}^2 = 9g^2\phi_{\rm g}$. Then the effective potential can be combined as

$$\Omega_{\rm g} = 72 g^2\phi_{\rm g}^2 - 16i\int\frac{{\rm d}^4p}{(2\pi)^4}\ln\left[-p^2 + M_{\rm g}^2\right], \tag{10}$$

and its finite temperature (T) and chemical potential (μ) extension is given by

$$\begin{aligned}
\Omega_{\rm g} &= 72 g^2\phi_{\rm g}^2 \\
&\quad + 16\int\frac{{\rm d}^3p}{(2\pi)^3}\left[E_{\rm g} + T\sum_{\pm}\ln(1 - e^{-\beta E_{\rm g}^{\pm}})\right],
\end{aligned} \tag{11}$$

where $E_{\rm g}^{\pm} = E_{\rm g} \pm \mu_{\rm g}$ with the chemical potential for gluons and $E_{\rm g} = \sqrt{p^2 + M_{\rm g}^2}$. The brief derivation of the effective potential is presented in Appendix A.

In this model, we treat the gluon condensate as the order parameter whose expectation value is determined by searching the minimum of the effective potential,

$$\frac{\partial\Omega_{\rm g}}{\partial\phi_{\rm g}} = 0. \tag{12}$$

The solution corresponds to the stational point of the effective potential, and the obtained equation can be reduced to

$$\phi_{\rm g} = \int\frac{{\rm d}^4p}{(2\pi)^4}\frac{-i}{p^2 - M_{\rm g}^2}. \tag{13}$$

This indicates the one-loop amplitude of the effective gluon propagator,

$$D_{\rm eff}^{\rm g}(p) = \frac{-i}{p^2 - M_{\rm g}^2}. \tag{14}$$

with the effective gluon mass $M_{\rm g}$. Thus the equation forms the self consistent system. The finite temperature and chemical potential extension of Eq. (13) becomes

$$\phi_{\rm g} = -\int\frac{{\rm d}^3p}{(2\pi)^3}\frac{1}{2E_{\rm g}}\left[1 - \sum_{\pm}\frac{1}{e^{\beta E_{\rm g}^{\pm}} - 1}\right]. \tag{15}$$

This is the gap equation for the gluon condensate which we will numerically solve in the next section.

B. Quark gap equation

To obtain effective quark contribution, we fist consider the four-fermion interaction in the two-flavor system following the discussion given in [24].

The QCD Lagrangian density is written by

$$\mathcal{L}_{\rm QCD} = \mathcal{L}^0_{\rm q} + \mathcal{L}_{\rm I} + \mathcal{L}_{\rm g}, \tag{16}$$

$$\mathcal{L}^0_{\rm q} = \overline{q}(i\partial\!\!\!/ - m)q, \tag{17}$$

$$\mathcal{L}_{\rm I} = g\overline{q}\gamma^\mu t^a q A^a_\mu, \tag{18}$$

The partition function can be expanded by using the Taylor series as

$$\begin{aligned}\mathcal{Z}_{\rm QCD} &= \int \mathcal{D}q \int \mathcal{D}A \exp\left[i\int {\rm d}^4x \mathcal{L}_{\rm QCD}\right] \\ &= \int \mathcal{D}q \int \mathcal{D}A e^{i\int {\rm d}^4x\mathcal{L}_0} \sum_{n=0}^{\infty} \frac{1}{n!}\left(i\int {\rm d}^4x \mathcal{L}_{\rm I}\right)^n, \end{aligned} \tag{19}$$

with $\mathcal{L}_0 = \mathcal{L}^0_{\rm q} + \mathcal{L}_{\rm g}$. Here we are interested only in the quark contribution, then focus on the amplitude,

$$\mathcal{Z}_{\rm q} \propto \int \mathcal{D}q \int \mathcal{D}A e^{i\int {\rm d}^4x\mathcal{L}^0_{\rm q}}\left[1 + \frac{1}{2}\left(ig\int {\rm d}^4x \mathcal{L}_{\rm I}\right)^2\right]. \tag{20}$$

The explicit form of the above equation is written by

$$\begin{aligned}\mathcal{Z}_{\rm q} \propto &\int \mathcal{D}q \int \mathcal{D}A e^{i\int {\rm d}^4x\mathcal{L}^0_{\rm q}} \\ &\times \left[1 + \frac{1}{2}\left(ig\int {\rm d}^4x \overline{q}\gamma^\mu t^a q A^a_\mu\right)^2\right]. \end{aligned} \tag{21}$$

The four-fermion contact interaction can be derived by assuming the gluons have sharp momentum peak around some specific energy scale in the propagator,

$$\left\langle A^a_\mu(x) A^b_\nu(y)\right\rangle_{\rm p} = \int \frac{{\rm d}^4p}{(2\pi)^4}\frac{-ig_{\mu\nu}\delta^{ab}}{p^2 + i\epsilon} e^{-ip\cdot(x-y)}. \tag{22}$$

The replacement $p^2 \to \eta^2_{\rm g}$ leads

$$\left\langle A^a_\mu(x) A^b_\nu(y)\right\rangle_{\rm const} = \frac{-ig_{\mu\nu}\delta^{ab}}{\eta^2_{\rm g}}\delta^{(4)}(x-y), \tag{23}$$

and it induces the four-fermion contact interaction

$$\begin{aligned}\mathcal{Z}_{\rm q} \simeq &\mathcal{N}_A \int \mathcal{D}q e^{i\int {\rm d}^4x\mathcal{L}_0} \\ &\times \left[1 + \frac{ig^2}{2\eta^2_{\rm g}}\int {\rm d}^4x \left(\overline{q}\gamma^\mu t^a q\right)\left(\overline{q}\gamma_\mu t^a q\right)\right]. \end{aligned} \tag{24}$$

with the over all factor $\mathcal{N}_A$ with respect to the gluon integration. Putting back the resulting term into the exponential using $1+\epsilon \simeq e^\epsilon$, we have the following effective Lagrangian for quarks

$$\mathcal{L}_{\rm eff} = \overline{q}(i\partial\!\!\!/ - m)q + \frac{g^2}{2\eta^2_{\rm g}}\left(\overline{q}\gamma^\mu t^a q\right)\left(\overline{q}\gamma_\mu t^a q\right). \tag{25}$$

This is how we derive the four-fermion contact interaction based on QCD with condensed gluons.

The applications of the mean field approximation, $\phi_{\rm q} \simeq \langle\bar{q}q\rangle$, after the Fiertz transformation gives

$$\tilde{\mathcal{L}}_{\rm q} = \bar{q}(i\partial\!\!\!/ - \hat{M})q - 2G(\phi^2_{\rm u} + \phi^2_{\rm d}), \tag{26}$$

where $G = 2g^2/(9\eta^2_{\rm g})$ and $\hat{M}$ is the diagonal matrix with $M_{\rm q} = m_{\rm q} - 4G\phi_{\rm q}$. One can evaluate the effective potential from the above mean-field form,

$$\begin{aligned}\Omega_{\rm q} &= 2G(\phi^2_{\rm u} + \phi^2_{\rm d}) \\ &\quad - 2N_c\sum_{\rm q}\int\frac{{\rm d}^3q}{(2\pi)^3}\left[E_{\rm q} + T\sum_{\pm}\ln\left(1 + e^{-\beta E^{\pm}_{\rm q}}\right)\right], \end{aligned} \tag{27}$$

with the number of colors $N_c(=3)$, $E^{\pm}_{\rm q} = E_{\rm q} \pm \mu_{\rm q}$ and $E_{\rm q} = \sqrt{q^2 + M^2_{\rm q}}$. From the stable condition of the effective potential, one has the gap equation,

$$\phi_{\rm q} = -{\rm tr}\int\frac{{\rm d}^4q}{(2\pi)^4}\frac{i}{q\!\!\!/ - M_{\rm q}}, \tag{28}$$

where the right hand side expresses the one-loop amplitude of the propagator for quarks

$$S^{\rm q}_{\rm eff}(q) = \frac{i}{q\!\!\!/ - M_{\rm q}}, \tag{29}$$

as seen in the gluon case. The finite temperature and chemical potential form becomes

$$\phi_{\rm q} = -4N_cM_{\rm q}\int\frac{{\rm d}^3q}{(2\pi)^3}\frac{1}{2E_{\rm q}}\left[1 - \sum_{\pm}\frac{1}{e^{\beta E^{\pm}_{\rm q}} + 1}\right]. \tag{30}$$

As frequently studied in quark effective model analyses, this gives the expectation values of the chiral condensates. Although this model is the same with the NJL model, we call it as the pure quark model in this letter to explicitly distinguish the model with gluon condensate.

C. Coupled equations

We have evaluated the effective potential both for the gluon and quark condensates above. One should note that the obtained forms compose the decoupled system since we set the effective coupling strength for four-fermion interaction as the constant. However, it is expected that the effective four-fermion interaction becomes weak at high temperature where the gluon condensate is as well expected to be small. Then we modify the form for the four-point coupling so that one can construct more reliable effective theory.

The constant property comes from the Eq. (23) in which the expectation value $\langle A^a_\mu A^b_\nu\rangle$ set to be constant. Here we modify this relation by

$$\left\langle A^a_\mu(x) A^b_\nu(y)\right\rangle = -ig_{\mu\nu}\delta^{ab}\cdot c\phi_{\rm g}\delta^{(4)}(x-y), \tag{31}$$

with the constant c, which enables us to incorporate the temperature dependence into the effective coupling. Note that the treatment in Eqs. (7) and (23) is essentially different; the former is obtained after the renormalization, and the latter still keeps the divergent contribution at $y = x$. The relation between these quantities are nontrivial, therefore we introduce the coefficient c in Eq. (31). Determining the coupling structure, we see the effective potential of the whole system,

$$\begin{aligned}\Omega =& 72g^2\phi_{\rm g}^2 + \frac{4}{9}g^2 c\phi_{\rm g}(\phi_{\rm u}^2+\phi_{\rm d}^2)\\ &+16\int\frac{{\rm d}^3p}{(2\pi)^3}\left[E_{\rm g}+T\sum_{\pm}\ln(1-e^{-\beta E_{\rm g}^{\pm}})\right]\\ &-6\sum_{\rm q}\int\frac{{\rm d}^3q}{(2\pi)^3}\left[E_{\rm q}+T\sum_{\pm}\ln\Big(1+e^{-\beta E_{\rm q}^{\pm}}\Big)\right], \quad (32)\end{aligned}$$

where $M_{\rm q} = m_{\rm q} - 8/9\, g^2 c\phi_{\rm g}\phi_{\rm q}$ appearing in the quasiparticle energy for quarks, $E_{\rm q}$. The coupled gap equations are calculated by the following simultaneous condition,

$$\frac{\partial\Omega}{\partial\phi_{\rm g}} = 0, \quad \frac{\partial\Omega}{\partial\phi_{\rm q}} = 0. \quad (33)$$

The above conditions give the explicit forms,

$$\begin{aligned}\phi_{\rm g} =& -\frac{c}{324}(\phi_{\rm u}^2+\phi_{\rm d}^2) - \int\frac{{\rm d}^3p}{(2\pi)^3}\frac{1}{2E_{\rm g}}\left[1-\sum_{\pm}n(E_{\rm g}^{\pm})\right]\\ &-\frac{c}{27}\sum_{\rm q}\int\frac{{\rm d}^3q}{(2\pi)^3}\frac{\phi_{\rm q}}{2E_{\rm q}}\left[1-\sum_{\pm}f(E_{\rm q}^{\pm})\right], \quad (34)\\ \phi_{\rm q} =& -4N_c M_{\rm q}\int\frac{{\rm d}^3q}{(2\pi)^3}\frac{1}{2E_{\rm q}}\left[1-\sum_{\pm}f(E_{\rm q}^{\pm})\right], \quad (35)\end{aligned}$$

with the distribution functions, $n(E) = (e^{\beta E}-1)^{-1}$ and $f(E) = (e^{\beta E}+1)^{-1}$, for bosons and fermions. These equations will give the expectation values of the gluon and chiral condensates.

III. SEPARATE MODELS

We have formulated the effective models for the gluon and chiral condensates in the previous section. We will now present actual numerical analyses concerning on the pure gluon and quark models.

A. Pure gluon model

Since the one-loop integral in the gap equation diverges, we need to introduce some regularization procedure to obtain finite model predictions. It is important to note that the gluon condensate becomes negative if we apply the three- or four-momentum cutoff schemes as usually introduced for the pure quark model, which leads the negative mass square $M_{\rm g}^2 < 0$. The negative mass square behaves badly in calculating the thermodynamical quantities, so we shall employ the dimensional regularization prescription which gives the positive gluon condensate [25], namely the positive mass square. The more detailed discussions on the sign of the condensate and the regularization prescriptions are presented in Apps. B and C. In the model with the dimensional regularization the gluon part has three parameters, the spacetime dimension D in the loop integral, the mass scale M_0, and the coupling constant for the strong interaction g. The coupling is chosen to be $g = 1.12$ from the consideration on the quark sector with $\eta_{\rm g} = 225$MeV, which will be discussed later. As for the remaining parameters, we set $D = 2.17$ and $M_0 = 67$MeV so that we have $M_g = 225{\rm MeV}(= \eta_{\rm g})$ at zero temperature and the critical temperature $T_c^{\rm g} = 270$MeV for pure gluon sector.

Figure 1 displays the numerical results of the gluon condensate. One sees that the condensate gradually decreases for low temperature, then suddenly drops around $T = 270$MeV. It should be mentioned that the gap equation allows a negative value for the solution, in which we regard unphysical mode so we set $\phi_{\rm g} = 0$ for the region corresponding to the case with the negative condensate. From the plots of the gluon condensate, we see that the curve actually shows the tendency of the symmetry restoration at finite temperature, which, we think, is the desired solution of the gap equation for the gluon condensate, Eq. (15).

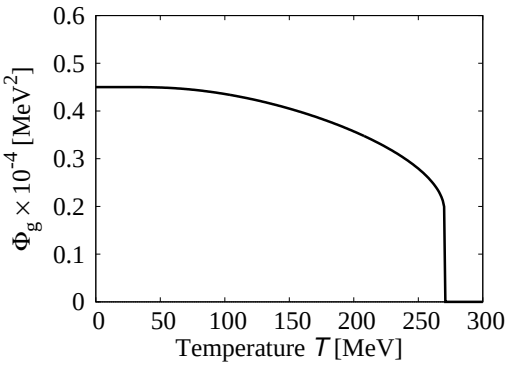

FIG. 1. The gluon condensate.

B. Pure quark model

When one sets the effective coupling strength for four-fermion interaction to be a constant, the model reduces to the NJL model as mentioned above, and which has five parameters: the gluon energy scale $\eta_{\rm g}$, three momentum cutoff $\Lambda_{\rm q}$, the coupling constant for the strong interac-

tion g, the current quark masses $m_{\rm u}$ and $m_{\rm d}$. We consider the isospin symmetric case $m_{\rm u} = m_{\rm d} (= m_{\rm q})$ since the mass difference between the up and down quarks is small comparing to the hadronic scale. Here we chose the value $m_{\rm q} = 5.5$MeV for the current quark mass, and $\eta_{\rm g} = 225$MeV for the gluon energy scale which is from the proton radius $r_{\rm P} \simeq 0.87$fm. We then fix the remaining parameters by $\Lambda_{\rm q} = 631$MeV and $g = 1.12$ so that the model reproduces the observed pion mass and decay constant, $m_\pi = 138$MeV and $f_\pi = 93$MeV following [19].

The numerical results of the chiral condensates for current quark mass $m_{\rm q} = 0$ and 5.5MeV are shown in Fig. 2. These are frequently drawn curves calculated in a lot of

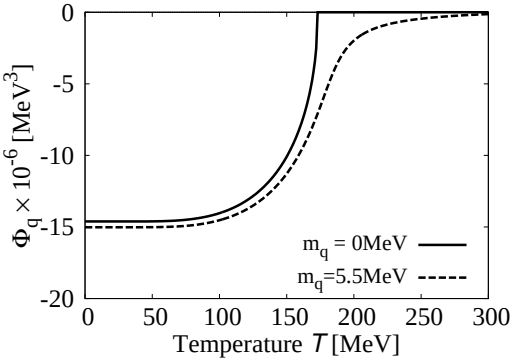

FIG. 2. The chiral condensate for $m_{\rm q} = 0$ and 5.5MeV with other parameters fixed.

preceding works, where the absolute value of the chiral condensate decreases at high temperature. The curve becomes smoother for the massive current quark mass case, which comes from the effect of the explicit symmetry breaking. The critical temperature of the chiral phase transition (defined by the maximum change of the condensate with respect to T and/or μ) for the above parameters set becomes $T_c^{\rm q} = 178$MeV, being close to the expected value from the lattice QCD simulations, $T_c^{\rm q} \simeq 175$MeV [26].

C. Comparisons with BEC and BCS

It may also be interesting to compare the results of the current model and the actual experimental data of the BEC state and the prediction from the BCS theory.

Figure 3 plots the temperature dependence on the gluon condensate and the condensed atoms in the BEC state. The dashed curve is the fitted result

$$\frac{N_0}{N} = 1 - \left(\frac{T}{T_c}\right)^3 - 4a\left(\frac{T}{T_c}\right)^{7/2}, \qquad (36)$$

with $a = 0.01$, where the transition temperature is $T_c = 142$nK for 87Rb [27]. One confirms that the two results basically show the resemblance, while curves a bit

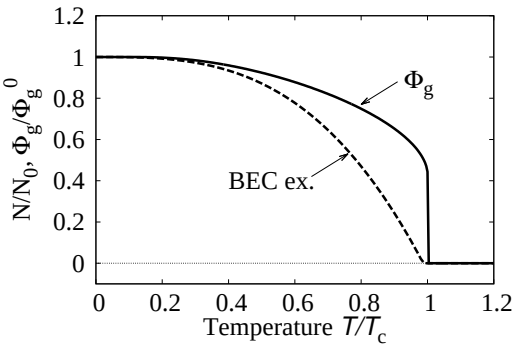

FIG. 3. Comparison with the fit of the BEC experimental data for the condensate atoms. The dashed curve is drawn by using the fitted formula, Eq (36) [27].

deviate. The deviation arises due to the difference between fitted formula and our gap equation. We note that the condensate drops rapidly at high temperature around T_c, which comes from the characteristic property of the Bose-Einstein distribution function, $n(E)$. The term can become infinitely large for $e^{\beta E_{\rm g}} \simeq 1$, then causes crucial effect on the solution at high temperature. This is the numerical reason on the drastic behavior of the condensate and its deviation from the BEC data at high temperature.

Although there exists the deviation from the expected behavior, we still think that the gap equation captures the phenomena of the phase transition at the satisfactory level for practical usage. We then regard Eq. (15) as the effective gap equation for the gluon condensate, then proceed the calculations on various thermodynamic quantities based on it.

We can as well check the similarity between the results of the chiral condensate and the BCS theory for superconductivity as seen in Fig. 4. The solid and dotted plots are the obtained chiral condensate in the pure quark sector for $m_{\rm q} = 0$ and 5.5MeV, and the dashed one is the prediction from the BCS gap equation,

$$\frac{\hbar\omega}{Nv} = \int_0^{\hbar\omega} {\rm d}\xi \, \frac{1}{E_\xi}\left[1 - \frac{2}{e^{\beta E_\xi} + 1}\right], \qquad (37)$$

where N is the number density, v is the potential of the system, and $E_\xi = \sqrt{\xi^2 + \Delta^2}$ with the BCS gap energy Δ [28]. The parameters in the BCS gap equation are chosen as $Nv = 0.3\hbar\omega$ with $\hbar\omega = 8.98 \times 10^{-3}$eV so that we have $T_c = 4.2$K for Hg. One notes that the lines of the chiral condensate for massless case and the BCS gap energy are very close as seen in the figure. This is due to the similarity of the quark gap equation and the BCS gap equation as obviously confirmed by Eqs. (30) and (37). The model with massive current quark gives smoother decrease with respect to T since the chiral condensate can not be restored completely with the non-zero current

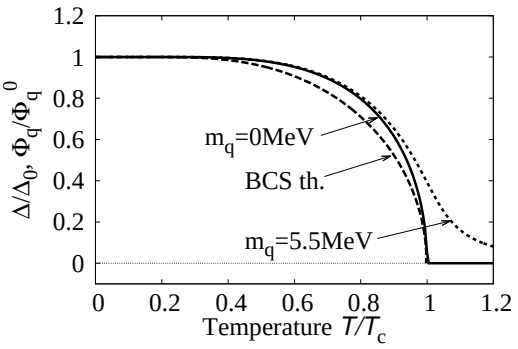

FIG. 4. Comparison with the result from the BCS theory for the gap equation, Eq (37), in superconductivity (dashed curve). The solid and dotted curves exhibit the results in the pure quark model for $m_u = 0$ and 5.5MeV with the other parameters fixed.

quark mass.

We have thus seen that both the gluon and chiral condensates resemble with the behavior of the BEC and BCS states. We believe this is indeed natural since our original motivations for the model constructions come from the analogies with these two typical phenomena in condensed matter physics.

IV. COUPLED MODEL

We have tested the condensates through the two gap equations separately in the previous section. Let us now discuss what happens when we consider the coupled system based on the simultaneous equations, Eqs. (34) and (35).

The coupled model has six parameters: the current quark masse $m_{\rm q}$, three-momentum cutoff $\Lambda_{\rm q}$, coupling constant for the strong interaction g, spacetime dimensions D, the mass scale M_0 and effective coupling coefficient c. We set these values by

$$m_{\rm q} = 5.5{\rm MeV}, \quad \Lambda_{\rm q} = 631{\rm MeV}, \quad g = 1.12,$$
$$D = 2.17, \quad M_0 = 67{\rm MeV}, \quad c = 0.439 \times 10^{-8}{\rm MeV}^{-4}.$$

Here we again present the reasoning on the above parameter choices. $m_{\rm q}$ is guessed from the data by Particle Data Group [29] around the scale ~ 1GeV. $\Lambda_{\rm q}$ and g are fitted so that the model leads the observed pion mass and decay constant $m_\pi = 138$MeV and $f_\pi = 93$MeV in the pure quark model following [19]. D and M_0 are set so as to produce the values $M_{\rm g} = 225$MeV at zero temperature and $T_c^{\rm g} = 270$MeV in the pure gluon model. c is chosen to make the effective quark mass to be $M_{\rm q} = 335$MeV at $T = 0$ and $\mu = 0$ in the coupled model. With these fitted parameters, we shall be studying the coupled system through solving the gap equations.

A. Gluon and chiral condensates

Figure 5 shows the obtained solutions for the gluon and chiral condensates. We note that the decrease of the

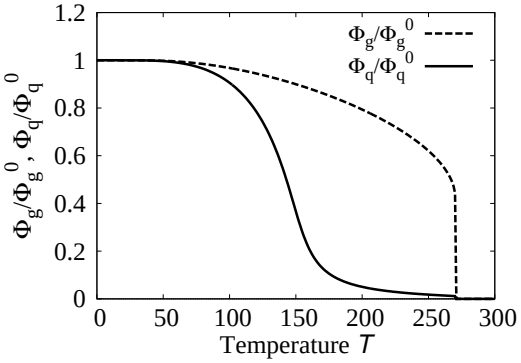

FIG. 5. Gluon and chiral condensates normalized by $\phi_{\rm g}^0 = (67{\rm MeV})^2$ and $\phi_{\rm q}^0 = (-247{\rm MeV})^3$.

chiral condensate starts at lower T compared to the pure quark model, while the solution for the gluon condensate is not affected in the coupled system. This can be understood by the following observations; the effective coupling for the four-fermion interaction gets weak at high temperature since the gluon condensate is smaller for high T, which lowers the critical temperature of the chiral phase transition. While the corresponding coupling on the gluon part is constant, and does not relate to the strength of the chiral condensate. Therefore, the critical behavior of the gluon condensate can not be affected by the quark part.

The obtained solutions may be reasonable in the current model study where the underlying assumption is that the quark condensate coming from the effective four-fermion interaction is driven by the gluon condensate. Considering the above mentioned property of the coupled equations, we will pay the attention to the difference on the quark system between the coupled and pure quark models in what follows.

B. Comparison with pure quark model

We see that the chiral condensate is influenced by the gluon condensate through the four-point interaction. It may be interesting to compare how the chiral condensate changes due to the gluon fields in the coupled system.

The influence of the gluon condensate effect is shown in Fig. 6, where the decrease starts at the lower temperature in the coupled model. As mentioned above, this is straightforward consequence of the weakened effective coupling. The critical temperature for the coupled model and pure quark model are $T_c^{\rm q} = 149$MeV and 178MeV,

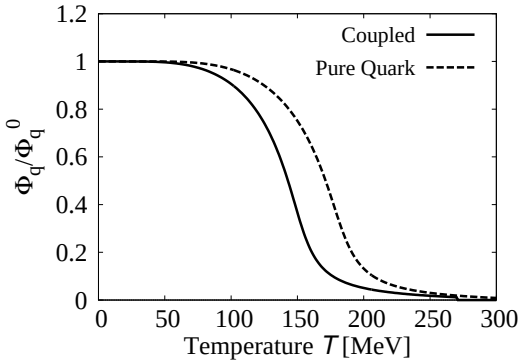

FIG. 6. The chiral condensates.

respectively. Thus we numerically confirm the change of the critical temperature being around 30MeV.

C. Pressure

It may be intriguing to study the pressures which are defined by

$$\mathcal{P}_{\rm g} = -\big[\Omega_{\rm g}(T,\mu) - \Omega_{\rm g}(0,0)\big], \tag{38}$$
$$\mathcal{P}_{\rm q} = -\big[\Omega_{\rm q}(T,\mu) - \Omega_{\rm q}(0,0)\big]. \tag{39}$$

So they are set by the difference of the effective potential from the value at $T = 0$ and $\mu = 0$.

The pressure from the gluon sector in the coupled models is displayed in the upper panel of Fig. 7. It should be noted that the gluon sector generates the same curve in the coupled and pure gluon models as discussed in Sec. IV A, therefore we only show the result of the coupled model for the gluon part. It is as well to be noted that the gap equation leads the unphysical solution with the negative mass square above $T_c^{\rm g} = 270$MeV, there we do not show the result since the thermodynamic quantities are not well defined above T_c in the current model analyses. The pressure of the gluon contribution normalized by $\pi^2T^4/90$ increases for low T, then decreases at high temperature. The decrease at high T numerically comes from our choice of the dimensional regularization method where the dimensions in the integral is smaller than four, then the contribution from the temperature dependent term is suppressed.

The interesting difference is seen in the lower panel of Fig. 7 where the pressures from the quark sector are plotted both in the coupled and pure quark models. The contribution becomes negative for low T and rises up for high T in the coupled model, while it monotonically increases with temperature in the pure quark model. This may indicate that the background gluon condensate tends to suppress the quark excitations in the confined state. On the other hand above $T_c^{\rm q}$, these two models produce the

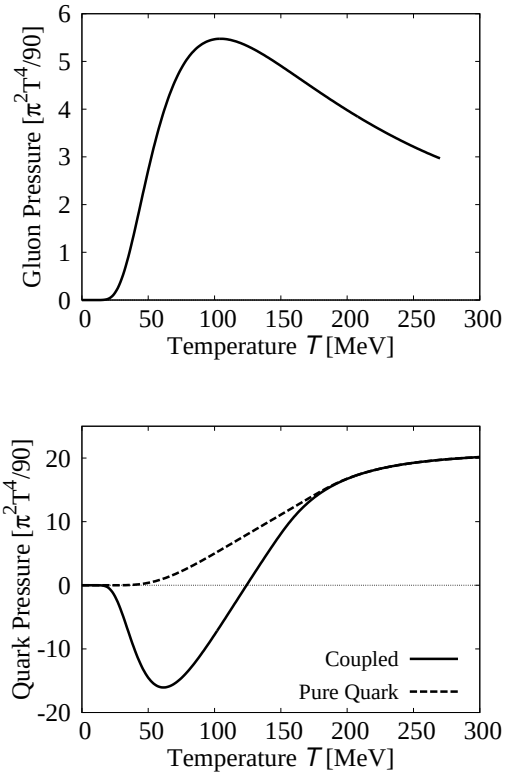

FIG. 7. Gluon and quark pressures.

same results since there the effective quarks turns into current quarks and the temperature contribution dominates the system.

D. Susceptibilities

The number density and susceptibility evaluated by

$$N_{\rm g} = -\frac{\partial\Omega_{\rm g}}{\partial\mu_{\rm g}}, \quad N_{\rm q} = -\frac{\partial\Omega_{\rm q}}{\partial\mu_{\rm q}}, \tag{40}$$
$$\chi_{\rm g} = -\frac{\partial^2\Omega_{\rm g}}{\partial\mu_{\rm g}^2}, \quad \chi_{\rm q} = -\frac{\partial^2\Omega_{\rm q}}{\partial\mu_{\rm q}^2}, \tag{41}$$

are important thermodynamic quantities which we will present in this subsection.

Figure 8 plots the number density for the gluon and quark sectors. It is seen that the curves for gluon sector and pure quark model indicate monotonic increase, while $N_{\rm q}$ in the coupled model exhibits different feature; the density becomes negative for low T then gets larger for high T. Although the negative number density seems to be unphysical which comes from the negative pressure, we get positive density being close to the one from the pure quark model above $T_c^{\rm q} \simeq 150$MeV as has been expected.

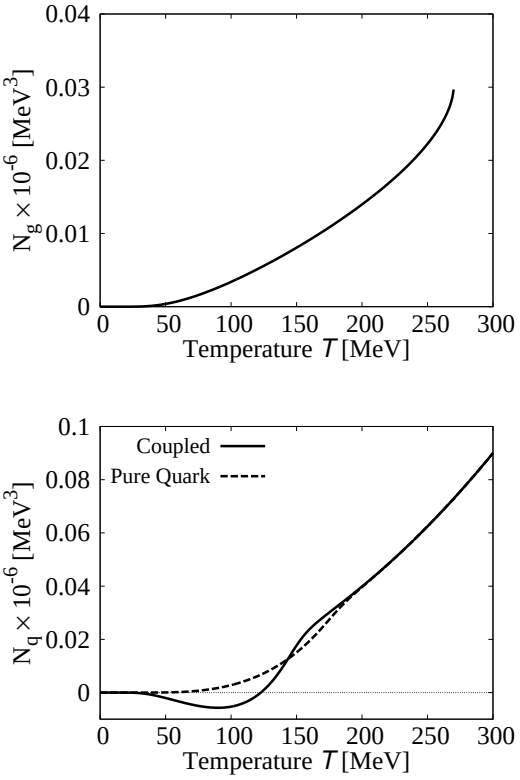

FIG. 8. Gluon and quark number densities.

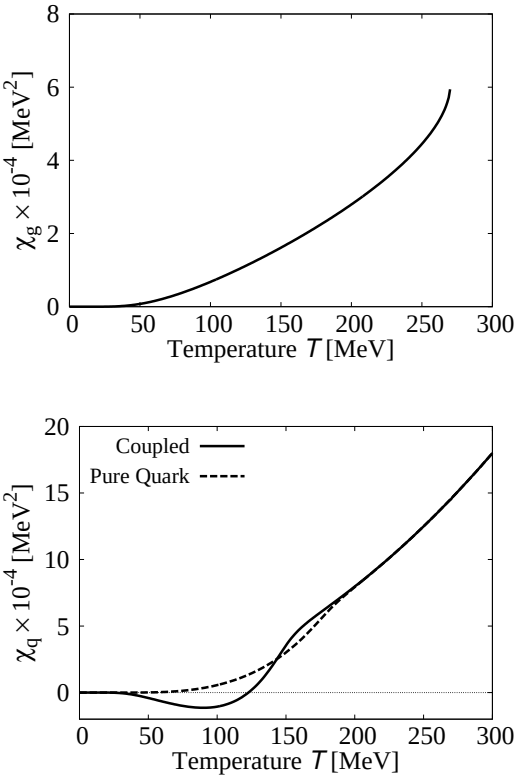

FIG. 9. Gluon and quark number susceptibilities.

The susceptibilities for the gluon and quark sectors are displayed in the upper and lower panels in Fig. 9. One notes a similar tendency on these results; the gluon sector and pure quark model draw the monotonically increasing lines, and the coupled model has negative value for low T.

We thus find the non-monotonic structure on the number density and susceptibility for the quark sector in the coupled model; the quark excitations are suppressed at low temperature. This is basically due to the change of the effective four-fermion coupling in the coupling system.

V. CHIRAL PHASE TRANSITION

We have seen the effect of the gluon condensate on the chiral condensate at finite temperature in the previous section. We think now it is interesting to study the system with finite quark chemical potential, in particular, the phase structure on the chiral phase transition.

A. Phase diagram of chiral condensate

We show how the phase transition of the chiral condensate has influence from the back ground gluon condensate in Fig. 10. The region of the broken phase shrinks

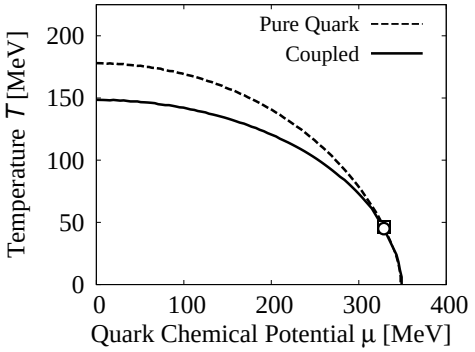

FIG. 10. Phase diagram for the chiral condensate. The circle (square) represents the critical point in the coupled (pure quark) model.

toward the lower temperature direction when one considers the coupled model, and there does not appear the

noticeable difference on the critical chemical potential for low T. This feature can easily be understood, since the gluon condensate becomes smaller at finite temperature. On the other hand, it is expected not to receive drastic change from the finite quark chemical potential $\mu_{\rm q}$, then the transition chemical potentials are the same between these models. It may be worth aligning the actual values of the critical chemical potential and temperature for two models. The coupled model gives $(\mu^{\rm q}_{\rm CP}, T^{\rm q}_{\rm CP}) = (329{\rm MeV}, 45{\rm MeV})$, and the pure quark model does $(\mu^{\rm q}_{\rm CP}, T^{\rm q}_{\rm CP}) = (329{\rm MeV}, 46{\rm MeV})$. Thus the change of the critical point is negligibly small comparing to the hadronic scale.

B. Susceptibilities at finite $\mu_{\rm q}$

We have previously calculated the quark number density and susceptibility in the temperature direction. We think it is also interesting to see the finite quark chemical potential behavior.

The comparison of the number density on the μ–T plane within two models is shown in Fig. 11. Nevertheless

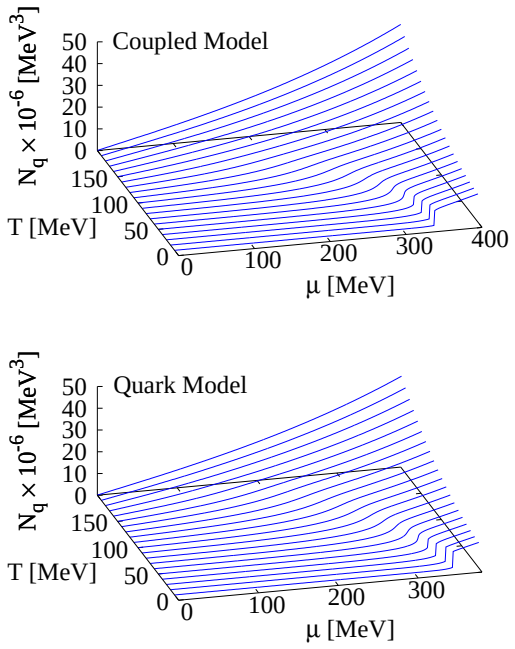

FIG. 11. Quark number density.

the deviation at finite T and zero $\mu_{\rm q}$ exists as observed in Figs. 8 and 9, the difference is not visually confirmed from the figure; then we may be able to conclude that the influence from the gluon condensate is not drastic in two models.

Also, the susceptibility is not considerably different as easily expected by the above results on the number density, which is shown in Fig. 12.

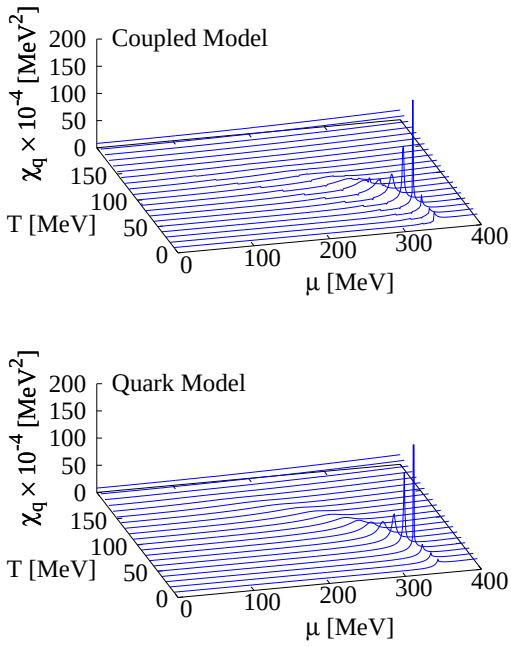

FIG. 12. Quark number susceptibility.

VI. CONCLUSIONS

We construct the effective model for the gluon and chiral condensates starting from QCD with the assumed gluon condensate in this paper. It is found that one can consider the gap equation of the gluon condensate through evaluating the effective potential. The solution shows desired behavior to some extent for low temperature region, while the transition near the critical temperature is more drastic compare to the experimental observation of the BEC state. This apparent discrepancy comes from the crucial distribution change at high temperature in the Bose-Einstein statistics for bosons which affects badly to the system of the gap equation. Therefore, we believe that the further considerations on the treatment of the gap equation for the gluon condensate, especially at high temperature near the transition temperature, should be given so that the model leads the better description on the phenomena of the phase transition.

Through the investigation of the coupled model, we studied how the gluon condensate affects to the chiral sector, particularly on the thermodynamic quantities and the critical phenomena. We find that the gluon condensate lowers the transition temperature, and suppress the quark excitations, i.e., the pressure, number density and susceptibility. Moreover, the gluon condensate effect reduces the critical temperature at high quark density. Here, it should be very important to note that the transition temperature and the location of the critical point are highly depends on the chosen regularization

produce and parameters as already searched in a lot of preceding works (see, e.g., [25]). Therefore it is necessary to carefully see the parameter dependence on the phase transition, which may be the future direction on this model analyses. On the other hand, the tendency that the gluon condensate suppresses the quark excitations for low temperature may be the universal feature of this kind of model with gluon condensate since the suppression is also seen in the PNJL model studies [23].

We think that the current model is still at the primitive level, since our purpose of the paper is to construct the model incorporating the gluon condensate based on QCD, then study the model behavior using the simplest form as the first step analysis. The crucial point of our simple model is the choice of the effective four coupling, Eq. (31), in which we set the coupling to be proportional to the gluon condensate. The numerical results shown in this paper are mainly come from the choice of the coupling. It may be needed to consider the form of the coupling as the function of the gluon condensate, e.g., $G = G(\phi_{\rm g})$, for the sake of constructing more realistic model. One more important point in our treatment is that we do not study the effect from the gluon chemical potential $\mu_{\rm g}$. In the real situation of the phase transition, the gluon chemical potential and quark chemical potential relate each other, then they should be treated simultaneously. This may also be future direction on this kind of approaches in considering the gluon and quark condensates.

The above mentioned future generalizations may be required and important. We believe that, since the current model may have the possibility of connecting effective models and the first principle theory of QCD, the further investigations based on this analysis are interesting.

ACKNOWLEDGMENTS

The author thanks to T. Inagaki and D. Kimura for discussions. The author is supported by Ministry of Science and Technology (Taiwan, ROC), through Grant No. MOST 103-2811-M-002-087.

Appendix A: The effective potential

The finite temperature extension of the one-loop contribution in the effective potential can be performed as follows.

In the imaginary-time formalism, we discretize the p_0-integral,

$$\int \frac{{\rm d}^4 p_E}{(2\pi)^4} F(p_{E0}, \mathbf{p}) \to T \sum_{n=-\infty}^{\infty} \int \frac{{\rm d}^3 p}{(2\pi)^3} F(\omega_n, \mathbf{p}), \quad \text{(A1)}$$

then we need to take the summation

$$\mathcal{F} = T \sum_{n=-\infty}^{\infty} \ln\left[\omega_n^2 + E^2\right], \quad \text{(A2)}$$

with $E^2 = p^2 + M^2$ and $\omega_n = 2n\pi T$ for bosons and $\omega_n = (2n+1)\pi T$ for fermions. We first differentiate the term with respect to E then divide by $2E$,

$$\frac{1}{2E}\frac{d\mathcal{F}}{dE} = T \sum_{n=-\infty}^{\infty} \frac{1}{\omega_n^2 + E^2}, \quad \text{(A3)}$$

here we can take the summation as

$$T \sum_{n=-\infty}^{\infty} \frac{1}{\omega_n^2 + E^2} = \frac{1}{2E}\left[1 - \frac{1}{e^{\beta E} - s}\right]. \quad \text{(A4)}$$

where $s = 1$ and -1 for the bosons and fermions, respectively. Thereafter the integration of $d\mathcal{F}/dE$ on E gives

$$\mathcal{F} = E + T\ln[1 - se^{-\beta E}], \quad \text{(A5)}$$

which leads Eqs. (11) and (27).

Appendix B: Sign of the condensates

We see that the gluon condensate becomes negative if we apply the three- or four-momentum cutoff method, which lead the negative effective mass square. This also happens in the scalar ϕ^4 theory, and we are going to discuss the issue of the sign using the ϕ^4 theory for simplicity.

Let's consider the following Lagrangian,

$$\mathcal{L}_{\phi^4} = \frac{1}{2}(\partial_\mu \phi)^2 - \frac{1}{4}\lambda\phi^4, \quad \text{(B1)}$$

where ϕ is the scalar field and λ is the four-point coupling. This gives the effective potential,

$$\Omega_{\phi^4} = \frac{1}{4}\lambda\phi^4 - \frac{i}{2}\int \frac{{\rm d}^4 p}{(2\pi)^4} \ln\left[-p^2 + M^2\right], \quad \text{(B2)}$$

with $M^2 = 3\lambda\phi^2$, then the gap equation ($\partial\Omega/\partial\phi = 0$) leads

$$\phi^2 = -3\int \frac{{\rm d}^4 p}{(2\pi)^4} \frac{i}{p^2 - M^2}. \quad \text{(B3)}$$

It is noted that ϕ^2 becomes negative if one introduces the four-momentum cutoff scale Λ as,

$$\phi^2 = -\frac{3}{16\pi^2}\left[\Lambda^2 - M^2 \ln\left(\frac{\Lambda^2 + M^2}{M^2}\right)\right] \quad \text{(B4)}$$

which leads the negative mass square for $\Lambda^2 \gg M^2$. To remedy the situation, we usually perform the renormalization through choosing a specific prescription, e.g., by using the $\overline{MS}$ scheme we have

$$\phi_{\rm r}^2 = -\frac{3}{16\pi^2}\left[M^2 \ln\frac{M^2}{\mu_{\rm r}^2}\right], \quad \text{(B5)}$$

with the renormalization scale $\mu_{\rm r}$. Note that for $\mu_{\rm r}^2 > M^2$, $\phi_{\rm r}^2$ becomes positive, then we can avoid the unwanted negative mass square.

It is worth mentioning that we can have the positive $M_{\rm g}^2$ as well for the gluon condensate at $T = 0$ if we apply the renormalization prescription. However, the system behaves badly at finite temperature when one considers the above mentioned renormalization. Here it is useful to employ the dimensional regularization, because it gives nice description both at zero and finite temperature contributions simultaneously thanks to applied analytic continuation. Therefore, for the sake of treating all the contributions under consistent way in our effective model analyses, we employ the dimensional regularization procedure for the gluon condensate.

On the other hand, we have for the fermion field,

$$\phi_{\rm q} = -{\rm tr}\int\frac{{\rm d}^4q}{(2\pi)^4}\frac{i}{\not{q} - M_{\rm q}} \tag{B6}$$

with $M_{\rm q} = m_{\rm q} - 4G\phi_{\rm q}$. Therefore one needs negative $\phi_{\rm q}$ in order to get the positive effective mass, and the three- or four-momentum cutoff way nicely works. This difference on the sign comes from the fact that fermion is a Grassmann number, which gives the negative sign in front of the third line of the effective potential, Eq. (32).

Appendix C: Regularization procedures

In the current model study, we employ the two types of regularization schemes so as to obtain the positive mass sign for $M_{\rm g}$ and $M_{\rm q}$.

For the gluon integration, as mentioned above, we apply the dimensional regularization which is defined by

$$\int\frac{{\rm d}^4p}{(2\pi)^4} \to M_0^{4-D}\int\frac{{\rm d}^Dp}{(2\pi)^D}, \tag{C1}$$

where D represents the spacetime dimensions, and the mass scale parameter M_0 is introduced to obtain correct mass dimensions for the integral.

The three-momentum cutoff scheme,

$$\int\frac{{\rm d}^4p}{(2\pi)^4} \to \frac{1}{2\pi^2}\int_{-\infty}^{\infty}\frac{{\rm d}p_0}{2\pi}\int_0^{\Lambda}{\rm d}pp^2 \tag{C2}$$

is the most frequently used method for the quark sector. We introduce the cutoff scale in the loop integral for zero temperature contribution, which gives the close curve to the BCS theory prediction as seen in Fig. 4.

[1] A. A. Belavin, A. M. Polyakov, A. S. Schwartz and Y. S. Tyupkin, Phys. Lett. B **59**, 85 (1975).
[2] C. G. Callan, Jr., R. F. Dashen and D. J. Gross, Phys. Rev. D **17**, 2717 (1978).
[3] A. I. Vainshtein, V. I. Zakharov, V. A. Novikov and M. A. Shifman, Sov. Phys. Usp. **25**, 195 (1982) [Usp. Fiz. Nauk **136**, 553 (1982)].
[4] T. Schäfer and E. V. Shuryak, Rev. Mod. Phys. **70**, 323 (1998).
[5] E. V. Shuryak and T. Sch?fer, Ann. Rev. Nucl. Part. Sci. **47**, 359 (1997).
[6] M. A. Shifman, A. I. Vainshtein and V. I. Zakharov, Nucl. Phys. B **147**, 448 (1979).
[7] L. J. Reinders, H. Rubinstein and S. Yazaki, Phys. Rept. **127**, 1 (1985).
[8] T. D. Cohen, R. J. Furnstahl, D. K. Griegel and X. m. Jin, Prog. Part. Nucl. Phys. **35**, 221 (1995).
[9] M. A. Shifman, Prog. Theor. Phys. Suppl. **131**, 1 (1998).
[10] F. J. Dyson, Phys. Rev. **75**, 1736 (1949).
J. S. Schwinger, Proc. Nat. Acad. Sci. **37**, 452 (1951).
[11] C. D. Roberts and A. G. Williams, Prog. Part. Nucl. Phys. **33**, 477 (1994).
[12] C. D. Roberts and S. M. Schmidt, Prog. Part. Nucl. Phys. **45**, S1 (2000).
[13] P. Maris and C. D. Roberts, Int. J. Mod. Phys. E **12**, 297 (2003).
[14] C. S. Fischer, J. Phys. G **32**, R253 (2006).
[15] Y. Nambu and G. Jona-Lasinio, Phys. Rev. **122**, 345 (1961); **124**, 246 (1961).
[16] J. Bardeen, L. N. Cooper and J. R. Schrieffer, Phys. Rev. **108**, 1175 (1957).
[17] U. Vogl and W. Weise, Prog. Part. Nucl. Phys. **27** (1991) 195.
[18] S. P. Klevansky, Rev. Mod. Phys. **64** (1992) 649.
[19] T. Hatsuda and T. Kunihiro, Phys. Rept. **247** (1994) 221.
[20] M. Huang, Int. J. Mod. Phys. E **14** (2005) 675.
[21] M. Buballa, Phys. Rept. **407** (2005) 205.
[22] K. Fukushima, Phys. Lett. B **591**, 277 (2004).
[23] K. Fukushima, Phys. Rev. D **77**, 114028 (2008) Erratum: [Phys. Rev. D **78**, 039902 (2008)].
[24] H. Kohyama, arXiv:1601.07832 [hep-ph].
[25] H. Kohyama, D. Kimura and T. Inagaki, Nucl. Phys. B **896**, 682 (2015).
[26] Y. Aoki, Z. Fodor, S. D. Katz and K. K. Szabo, Phys. Lett. B **643**, 46 (2006).
[27] E. A. L. Henn, J. A. Seman, G. B. Seco, E. P. Olimpio, P. Castilho, G. Roati, D. V. Magalhaes, K. M. F. Magalhaes, V. S. Bagnato, Braz. J. Physics, 38, no.2, 279 (2008).
[28] M. Tinkham, "Introduction to superconductivity," New York: McGraw-Hill (1975).
[29] K. A. Olive *et al.* [Particle Data Group Collaboration], Chin. Phys. C **38** (2014) 090001.